Synthesis and Spectroscopic Characterization of Halodimethyl(*O*-alkyl dithiocarbonato)tellurium(IV) Compounds. Crystal Structures of $Me_2TeCl[S_2COEt]$ and $Me_2TeI[S_2CO(i\text{-}Pr)]$

John E. Drake,* Robert J. Drake, Layla N. Khasrou, and Raju Ratnani†

Department of Chemistry and Biochemistry, University of Windsor, Windsor, Ontario, Canada N9B 3P4

Received September 8, 1995[⊗]

O-Alkyl dithiocarbonate (xanthate) derivatives of halodimethyltellurium(IV), $Me_2TeX[S_2COR]$, where R = Me, Et, and *i*-Pr and X = Cl, Br, and I, have been prepared in 75−88% yields by the reaction of the potassium salt of the appropriate dithiocarbonic acid with dimethyltellurium dihalide in equimolar ratio. The compounds were characterized by infrared, Raman, and ^1H, ^{13}C, and ^{125}Te NMR spectroscopy. The crystal structures of $Me_2TeCl[S_2COEt]$ (**2**) and $Me_2TeI[S_2CO(i\text{-}Pr)]$ (**9**) were determined. $Me_2TeCl[S_2COEt]$ (**2**), which crystallizes in the monoclinic space group $P2_1/a$ (No. 14), has the cell parameters $a = 9.583(2)$ Å, $b = 10.264(3)$ Å, $c = 22.502(2)$ Å, $\beta = 97.86(1)°$, $V = 2192.4(8)$ Å^3, and $Z = 8$, and $Me_2TeI[S_2CO(i\text{-}Pr)]$ (**9**), which crystallizes in the triclinic space group $P\bar{1}$ (No. 2), has the cell parameters $a = 11.332(5)$ Å, $b = 11.83(2)$ Å, $c = 10.19(2)$ Å, $\alpha = 94.8(2)°$, $\beta = 105.53(7)°$, $\gamma = 85.10(7)°$, $V = 1309(3)$ Å^3, and $Z = 2$. The immediate environment about tellurium in both molecules can be described as that of a sawhorse structure in which the lone pair is apparently stereochemically active and occupying an equatorial position in a distorted trigonal bipyramid. The two methyl groups occupy the other equatorial positions with a sulfur atom of the dithiocarbonate group and a halogen atom occupying the axial positions. However, intermolecular Te--I interactions between the two molecules of the asymmetric unit of **9** suggest that it is better described as dimeric, whereas the intermolecular Te--Cl associations in **2** lead to polymeric strands rather than dimers. Supramolecular associations are discussed in terms of Pauling bond orders.

Introduction

Extensive studies have been carried out on *O*-alkyl dithiocarbonates (xanthates) as ligands, particularly with transition metals,[1] but only relatively recently have there been reports on tellurium derivatives.[2−9] The current interest in tellurium complexes with sulfur ligands is illustrated by the comprehensive review by King *et al.* on stereochemical aspects and supramolecular associations.[10] Similar intermolecular halogen interactions in tellurium halides are well established[11] and there has been a report of the structure of the mixed haloxanthate tellurium(II) derivative, $Te[S_2COEt]Br$,[8] as well as our recent report on structures of halomonothiocarbamate derivatives of tellurium(IV).[12] As part of a general study of the structure reactivity relationships in compounds containing a tellurium-sulfur bond,[12−18] we recently described the formation of a number of diorganobis(dithiocarbonato)tellurium(IV) derivatives.[19] This paper deals with the synthesis and spectroscopic properties of a variety of halodimethyl(*O*-alkyl dithiocarbonato)-tellurium(IV) derivatives, $Me_2TeX[S_2COR]$, where R = Me, Et, and *i*-Pr and X = Cl, Br, and I, as well as the crystal structures of $Me_2TeCl[S_2COEt]$ (**2**) and $Me_2TeI[S_2CO(i\text{-}Pr)]$ (**9**). In response to the continuing interest in the calculation of the vibrational frequencies of xanthates,[20] we include a normal coordinate analysis of the $Me_2TeX[S_2COMe]$ series which confirms the extensive mixing among the force constants in modes involving the S_2COC core.

Experimental Section

Materials. $TeCl_4$ and Me_4Sn were obtained from Aldrich. $TeBr_4$ and Me_2TeI_2 were obtained from Alfa and Organometallics, Inc., respectively. Me_2TeCl_2 and Me_2TeBr_2 were prepared by the adaption of the method described in the literature for the preparation of Ph_2TeCl_2[21] by the reaction of $TeCl_4$ or $TeBr_4$ with Me_4Sn in toluene at 60 °C under reflux for 4 h. Sodium and potassium salts of *O*-methyl,

* Author to whom correspondence should be addressed.
† Current address: Department of Chemistry, Dayanand College, Ajmer, 305 001, India.
⊗ Abstract published in *Advance ACS Abstracts,* April 1, 1996.

(1) Burns, R. P.; McCullough, F. P.; McAuliffe, C. A. *Adv. Inorg. Chem. Radiochem.* **1980**, *23*, 211, and Zeiss, W. C. *Acad. R. Sci. (Copenhagen)* **1815**, *1*, 1.
(2) Wieber, M.; Schmidt, E.; Burschka, C. *Z. Anorg. Allg. Chem.* **1985,** *525,* 127.
(3) Singh, A. K.; Basumatary, J. K.; Singh, T. P.; Padmanabhan, B. *J. Organomet. Chem.* **1992,** *424,* 33.
(4) Dakternieks, D.; Di Giacomo, R.; Gable, R. W.; Hoskins, B. F. *J. Am. Chem. Soc.* **1988,** *110,* 6753.
(5) Husebye, S.; Maartmann-Moe, K.; Mikalsen, O. *Acta Chem. Scand.* **1989,** *43,* 754.
(6) Hauge, S.; Vikane, O. *Acta Chem. Scand.* **1985,** *A39,* 553.
(7) Husebye, S. *Acta Chem. Scand.* **1967,** *21,* 42.
(8) Gable, R. W.; Hoskins, B. F.; Steen, R. J.; Winter, G. *Inorg. Chim. Acta* **1983,** *72,* 173.
(9) Hoskins, B. F.; Tiekink, E. R. T.; Winter, G. *Inorg. Chim. Acta* **1985,** *96,* L79.
(10) Haiduc, I.; King, R. B.; Newton, M. G. *Chem. Rev.* **1994,** *94,* 301.
(11) Wells, A. F. *Structural Inorganic Chemistry,* 4th ed.; Oxford University Press: Oxford, England, 1975; p 578.
(12) Drake, J. E.; Khasrou, L. N.; Mislankar, A. G.; Ratnani, R. *Inorg. Chem.* **1994**, *33*, 6154.
(13) Drake, J. E.; Khasrou, L. N.; Mislankar, A. G.; Ratnani, R. *Can. J. Chem.* **1994**, *72*, 1328.
(14) Bailey, J. H. E.; Drake, J. E. *Can. J. Chem.* **1993**, *71*, 41.
(15) Bailey, J. H. E.; Drake, J. E.; Wong, M. L. Y. *Can. J. Chem.* **1991**, *69*, 1948.
(16) Bailey, J. H. E.; Drake, J. E.; Sarkar, A. B. Wong, M. L. Y. *Can. J. Chem.* **1989**, *67*, 1735.
(17) Drake, J. E. Wong, M. L. Y. *J. Organomet. Chem.* **1989**, *377*, 43.
(18) Chadha, R. K.; Drake, J. E.; McManus, N. T.; Quinlan, B. A.; Sarkar, A. B. *Organometallics* **1987**, *6*, 813.
(19) Bailey, J. H. E.; Drake, J. E.; Khasrou, L. N.; Yang, J. *Inorg. Chem.* **1995**, *34*, 124.
(20) Colthrup, N. B.; Powell, L. P. *Spectrochim. Acta* **1987,** *43A,* 317.
(21) Paul, R. C.; Bhasin, K. K.; Chadha, R. K. *J. Inorg. Nucl. Chem.* **1975**, *37*, 2337.

S0020-1669(95)01173-6 CCC: $12.00

ethyl, and isopropyl dithiocarbonic (xanthic) acids were prepared as described previously.[22] All solvents were dried and distilled prior to use and all reactions were carried out under moisture free conditions. Elemental analyses were performed at Guelph Chemical Laboratories, Ontario, Canada.

Preparation of Chlorodimethyl(*O*-methyl dithiocarbonato)tellurium(IV), $Me_2TeCl[S_2COMe]$ (1). Typically, dimethyltellurium dichloride (0.23 g, 1.0 mmol) and the potassium salt of *O*-methyl dithiocarbonate (0.15 g, 1.0 mmol) were placed in a round-bottom flask and dissolved in dichloromethane (20 mL). The mixture was kept in an ice-bath and stirred for 2−3 h and then filtered to remove KCl and unreacted materials. The solution was evaporated to dryness to give a white solid, which was recrystallized from a chloromethane/*n*-hexane mixture to give $Me_2TeCl[S_2COMe]$ (**1**): white needle-shaped crystals, 0.263 g, yield 88%, mp 81−83 °C. Anal. Calcd for $C_4H_9OS_2ClTe$: C, 15.99; H, 3.02. Found: C, 15.89; H, 2.93. Similarly were formed $Me_2TeCl[S_2COEt]$ (**2**) (white crystals, yield 82%, mp 58−59 °C. Anal. Calcd for $C_5H_{11}OS_2ClTe$: C, 19.11; H, 3.53. Found: C, 18.45; H, 3.31) and $Me_2TeCl[S_2CO(i\text{-}Pr)]$ (**3**) (white crystals, yield 85%, mp 56−58 °C). Only for **2** was it possible to isolate X-ray quality crystals.

Preparation of Bromodimethyl(*O*-ethyl dithiocarbonato)tellurium(IV), $Me_2TeBr[S_2COEt]$ (5). Typically, the potassium salt of *O*-ethyl dithiocarbonate (0.16 g, 1.0 mmol) and dimethyltellurium dibromide (0.32 g, 1.0 mmol) were placed in a round-bottom flask and dissolved in dichloromethane (20 mL). A rapid reaction ensued with the colorless solution becoming bright yellow. The mixture was stirred for 2 h at approximately 0 °C and then filtered to remove KBr and unreacted materials. The solvent was reduced to 2 mL, *n*-hexane (approximately 2 mL) was added, and the solution was left overnight in the refrigerator at −6 °C. A pale yellow powder was formed which was dried under vacuum. Thus was formed $Me_2TeBr[S_2COEt]$ **(5)**: pale yellow powder, 0.22 g, yield 77%, mp 68−70 °C. Anal. Calcd for $C_5H_{11}OS_2BrTe$: C, 16.74; H, 3.09. Found: C, 17.16; H, 2.99. Similarly were formed $Me_2TeBr[S_2COMe]$ **(4)** (pale yellow powder, yield 81%, mp 76−78 °C. Anal. Calcd for $C_4H_9OS_2BrTe$: C, 13.94; H, 2.63. Found: C, 13.76; H, 2.89) and $Me_2TeBr[S_2CO(i\text{-}Pr)]$ **(6)** (pale yellow needle-like crystals, yield 81%, mp 69−71 °C). Despite extensive efforts, X-ray quality crystals were not obtained.

Preparation of Iododimethyl(*O*-isopropyl dithiocarbonato)tellurium(IV). $Me_2TeI[S_2CO(i\text{-}Pr]$ (9). Typically, the potassium salt of *O*-isopropyl dithiocarbonate (0.08 g, 0.5 mmol) was added to a solution of dimethyltellurium diiodide (0.21 g, 0.5 mmol) in dichloromethane (20 mL). The color of the solution became yellow-green within a few minutes of the addition of the salt. The mixture was stirred for 2 h at approximately 0 °C and then filtered to remove KI and unreacted materials. The solvent was pumped off to leave a yellow solid, which was redissolved in a dichloromethane (2 mL) and *n*-hexane (2 mL) mixture before the solution was left overnight in the refrigerator at −6 °C. The yellow crystals that formed were decanted and then dried under vacuum. Thus was formed $Me_2TeI[S_2CO(i\text{-}Pr]$ **(9)**: yellow block-shaped crystals, 0.16 g, yield 77%, mp 79−80 °C. Anal. Calcd for $C_6H_{13}OS_2ITe$: C, 17.17; H, 3.12. Found: C, 18.13; H, 3.27. Similarly was formed $Me_2TeI[S_2COMe]$ **(7)** (yellow oil/paste, yield 76%) and $Me_2TeI[S_2COEt]$ **(8)** (yellow powder, yield 77%, mp 52−53 °C). Anal. Calcd for $C_5H_{11}OS_2ITe$: C, 14.80; H, 2.73. Found: C, 14.08; H, 2.65. Only for **9** was it possible to isolate X-ray quality crystals. If stored at room temperature, compound **7** began to darken within a matter of hours, gradually taking on the color of Me_2TeI_2.

Physical Measurements. The infrared spectra were recorded on a Nicolet 5DX FT spectrometer as KBr pellets and far-infrared spectra on a Bomem IR spectrometer between polyethylene films as Nujol mulls. Raman spectra were recorded using samples in sealed capillary tubes on a Spectra-Physics 164 spectrometer using the 5145-Å exciting line of an argon ion laser. ^1H and ^{13}C NMR spectra were recorded on a Bruker 300 FT NMR spectrometer in $CDCl_3$ solutions using Me_4Si as internal standard. ^{125}Te NMR spectra were recorded on a Bruker 200 FT NMR spectrometer in $CDCl_3$ using Me_2Te as external standard. The melting and decomposition points were recorded on a Fisher-Johns apparatus.

(22) Magee, R. J.; O'Connor, M. J. *Inorg. Chim. Acta* **1971**, *5*, 554.

Table 1. Crystallographic Data for $Me_2TeCl[S_2COEt]$ (**2**) and $Me_2TeI[S_2CO(i\text{-}Pr]$ (**9**)

	$Me_2TeCl[S_2COEt]$ (**2**)	$Me_2TeI[S_2CO(i\text{-}Pr)]$ (**9**)
chem formula	$C_5H_{11}OS_2ClTe$	$C_6H_{13}OS_2TeI$
fw, g mol^{-1}	311.82	419.80
a, Å	9.583(2)	11.332(5)
b, Å	10.264(3)	11.83(2)
c, Å	22.502(2)	10.19(2)
α, deg	90.00	94.8(2)
β, deg	97.86(1)	105.53(7)
γ, deg	90.00	85.10(7)
V, Å^3	2192.4(8)	1309(3)
space group	$P2_1/a$ (No. 14)	$P\bar{1}$ (No. 2)
Z	8	4
ρ_{calc}, g cm^{-3}	1.90	2.13
T, °C	23	23
μ, cm^{-1}	32.79	49.10
R^a	0.0417	0.0476
$R_w{}^b$	0.0348	0.0419

$^a R = \sum||F_o| - |F_c||/\sum F_o|$. $^b R_w = [(\sum w(|F_o| - |F_c|)^2/\sum wF_o^2)]^{1/2}$.

X-ray Crystallographic Analysis. A white needle-shaped crystal of $Me_2TeCl[S_2COEt]$ **(2)**, and a yellow block crystal of $Me_2TeI[S_2CO(i\text{-}Pr)]$ **(9)** were sealed in thin-walled glass capillaries and mounted on a Rigaku AFC6S diffractometer, with graphite-monochromated Mo Kα radiation.

Cell constants and an orientation matrix for data collection, obtained from a least-squares refinement using the setting angles of 15 carefully centered reflections in the range $25.71 < 2\theta < 31.63$ (for **2**) and $12.88 < 2\theta < 26.37$ (for **9**), corresponded to monoclinic (**2**) and triclinic (**9**) cells whose dimensions are given in Table 1. On the basis of systematic absences ($h0l$, $h = 2n + 1$; $0k0$, $k = 2n + 1$) (for **2**), packing considerations, statistical analyses of intensity distributions, and the successful solution and refinement of the structures, the space groups were determined to be $P2_1/a$ (No. 14) for **2** and $P\bar{1}$ (No. 2) for **9**.

The data were collected at a temperature of 23 ± 1 °C using the $\omega-2\theta$ scan technique to a maximum 2θ value of 50.0°. The ω scans of several intense reflections, made prior to data collection, had average widths at half-height of 0.35 (**2**) and 0.46° (**9**) with takeoff angles of 6.0° each. Scans of $(1.57 + 0.30 \tan \theta)°$ were made at a speed of 16.0°/min (in ω) for both **2** and **9**. The weak reflections ($I < 10.0\sigma(I)$) were rescanned (maximum of 3 rescans), and the counts were accumulated to assure good counting statistics. Stationary background counts were recorded on each side of the reflection. The ratio of peak counting time to background counting time was 2:1. The diameter of the incident beam collimator was 1.0 mm, and the crystal to detector distance was 285 mm.

Of the 4374 (**2**) or 4863 (**9**) reflections which were collected, 4112 (**2**) or 4608 (**9**) were unique ($R_{int} = 0.069$ and 0.037 for **2** and **9**, respectively). The intensities of three representative reflections which were measured after every 150 reflections remained constant throughout data collection indicating crystal and electronic stability (no decay corrections were applied).

The linear absorption coefficients for Mo Kα were 32.79 cm^{-1} (for **2**) and 49.10 cm^{-1} (for **9**). An empirical absorption correction, based on azimuthal scans of several reflections, was applied for each, which resulted in transmission factors ranging from 0.64 to 1.00 (for **2**) and from 0.56 to 1.00 (for **9**). The data were corrected for Lorentz and polarization effects.

The structures were solved by direct methods.[23] The non-hydrogen atoms were refined anisotropically and the hydrogen atoms were included in their idealized positions with C−H set at 0.95 Å and with isotropic thermal parameters set at 1.2 times that of the carbon atom to which they were attached. The final cycle of full-matrix least-squares refinement[24] was based on 2358 (**2**) and 2963 (**9**) observed reflections ($I > 3.00\sigma(I)$) and 182 (**2**) and 200 (**9**) variable parameters and converged (largest parameter shift was 0.0005 times its esd) with

(23) Sheldrick, G. M. *Crystallographic Computing 3*; Sheldrick, G. M., Kruger, C., Goddard, R., Eds.; Oxford University Press: Oxford, England, 1985; p 175.

Table 2. Final Fractional Coordinates and *B*(eq) Values for Non-Hydrogen Atoms of $Me_2TeCl[S_2COEt]$ **(2)** with Standard Deviations in Parentheses

atom	x	y	z	*B*(eq), Å^2
Te(1)	0.25021(7)	0.16118(6)	0.43930(3)	2.53(3)
Te(2)	0.26518(7)	0.06529(6)	0.09114(3)	3.02(3)
Cl(1)	0.4805(3)	0.2297(2)	0.5139(1)	3.8(1)
Cl(2)	0.0471(3)	0.2220(3)	0.0555(1)	5.2(2)
S(1)	0.0427(3)	0.0522(3)	0.3784(1)	4.1(1)
S(2)	0.1532(3)	0.2533(3)	0.2996(1)	4.2(1)
S(3)	0.4549(3)	−0.1025(3)	0.1152(1)	4.9(2)
S(4)	0.3388(4)	−0.0277(3)	0.2280(1)	5.4(2)
O(1)	−0.0530(7)	0.0854(7)	0.2704(3)	3.8(4)
O(2)	0.548(1)	−0.189(1)	0.2163(4)	7.1(5)
C(1)	0.394(1)	0.052(1)	0.3947(5)	4.2(6)
C(2)	0.229(1)	0.022(1)	0.5079(4)	3.3(5)
C(3)	0.045(1)	0.135(1)	0.3114(4)	3.0(5)
C(4)	−0.073(1)	0.137(1)	0.2093(5)	4.3(6)
C(5)	−0.192(1)	0.065(1)	0.1740(5)	5.9(7)
C(6)	0.108(1)	−0.080(1)	0.0939(5)	4.6(6)
C(7)	0.285(1)	0.041(1)	−0.0027(4)	4.6(6)
C(8)	0.449(1)	−0.108(1)	0.1920(5)	4.3(6)
C(9)	0.563(2)	−0.225(2)	0.2815(8)	8(1)
C(10)	0.668(2)	−0.149(2)	0.3143(8)	10(1)

[a] $B(\text{eq}) = 8\pi^2/3[U_{11}(aa^*)^2 + U_{22}(bb^*)^2 + U_{33}(cc^*)^2 + 2U_{12}aa^*bb^*(\cos\gamma) + 2U_{13}aa^*cc^*(\cos\beta) + U_{23}bb^*cc^*(\cos\alpha)]$.

unweighted and weighted agreement factors of $R = \sum||F_o| - |F_c||\sum|F_o| = 0.0417$ (for **2**) and 0.0476 (for **9**) and $R_w = [(\sum w(|F_o| - |F_c|)^2/\sum wF_o^2)]^{1/2} = 0.0348$ (for **2**) and 0.0476 (for **9**).

The standard deviation of an observation of unit weight[25] was 1.86 (for **2**) and 2.48 (for **9**). The weighting scheme was based on counting statistics and included a factor ($p = 0.003$ (**2**) and 0.009 (**9**)) to downweight the intense reflections. Plots of $\sum w(|F_o| - F_c)^2$ vs $|F_o|$, reflection order in data collection, $(\sin\theta)/\lambda$, and various classes of indices showed no unusual trends. The maximum and minimum peaks on the final difference Fourier map corresponded to +0.89 and −0.87 e/Å^3, respectively, for **2** and +1.54 and −1.43 e/Å^3, respectively, for **9**.

Neutral-atom scattering factors were taken from Cromer and Waber.[26] Anomalous dispersion effects were included in F_c;[27] the values for $\Delta f'$ and $\Delta f''$ were those of Cromer.[28] All calculations were performed using the TEXSAN[29] crystallographic software package of Molecular Structure Corp.

The final atomic coordinates and equivalent isotropic thermal parameters (Tables 2 and 3) are given respectively for **2** and **9** for the non-hydrogen atoms and important distances and bond angles in Tables 4 and 5. The molecular structures of the asymmetric units that are shown as ORTEP diagrams in Figures 1 and 2 do not include the secondary inter- or intramolecular interactions. These secondary interactions are displayed in Figures 3 and 4. Additional crystallographic data are available as supporting information.

Calculation of Pauling Bond Order. The formula proposed by Pauling[30] for calculating the bond orders of partial bonds is given by $d_n - d = -0.60 \log n$, where d_n is the bond length for bond number n and d is the length of the single bond of the same type. On the basis of the C−C single bond of 1.54 Å, Pauling's formula gives a bond length of 1.36 Å for $n = 2$, 1.72 Å for $n = 0.5$, and 1.90 Å for $n = 0.25$. These give percentage increases in bond length for the partial bonds of approximately 12 and 23% respectively for $n = 0.5$ and 0.25. It is reasonable to assume that similar relationships relating bond order

Table 3. Final Fractional Coordinates and *B*(eq) Values for Non-Hydrogen Atoms of $Me_2TeI[S_2CO(i\text{-}Pr)]$ **(9)** with Standard Deviations in Parentheses

atom	*x*	*y*	*z*	*B*(eq), Å^2
I(1)	1.07169(7)	0.76564(9)	0.0291(1)	4.47(5)
I(2)	1.10195(8)	0.71835(9)	0.5170(1)	4.54(4)
Te(1)	0.90071(7)	0.85415(8)	0.20577(9)	3.41(4)
Te(2)	1.18032(7)	0.54799(8)	0.30693(8)	3.20(4)
S(1)	0.7756(3)	0.9516(3)	0.3577(4)	4.4(2)
S(2)	0.6584(3)	0.7381(4)	0.2197(4)	5.3(2)
S(3)	1.2363(3)	0.3990(3)	0.1369(3)	4.1(2)
S(4)	1.4628(3)	0.4942(4)	0.3252(4)	4.5(2)
O(1)	0.5976(8)	0.8754(9)	0.413(1)	5.2(5)
O(2)	1.4491(6)	0.3368(8)	0.1231(8)	4.0(4)
C(1)	0.782(1)	0.920(1)	0.024(1)	4.5(7)
C(2)	1.017(1)	0.993(1)	0.274(1)	4.5(7)
C(3)	0.669(1)	0.847(1)	0.328(1)	3.9(6)
C(4)	0.489(1)	0.811(1)	0.406(2)	7(1)
C(5)	0.381(2)	0.865(2)	0.309(2)	11(1)
C(6)	0.478(2)	0.815(2)	0.546(2)	9(1)
C(7)	1.218(1)	0.430(1)	0.462(1)	4.3(7)
C(8)	0.993(1)	0.511(1)	0.223(1)	4.3(6)
C(9)	1.395(1)	0.409(1)	0.197(1)	2.8(5)
C(10)	1.587(1)	0.322(1)	0.159(1)	3.9(6)
C(11)	1.632(1)	0.402(2)	0.084(2)	6.4(9)
C(12)	1.614(1)	0.200(1)	0.118(1)	5.4(8)

[a] $B_{eq} = 8\pi^2/3[U_{11}(aa^*)^2 + U_{22}(bb^*)^2 + U_{33}(cc^*)^2 + 2U_{12}aa^*bb^*(\cos\gamma) + 2U_{13}aa^*cc^*(\cos\beta) + U_{23}bb^*cc^*(\cos\alpha)]$.

Table 4. Important Interatomic Distances (Å) and Angles (deg) for $Me_2TeCl[S_2COEt]$ (2)

Te(1)−Cl(1)	2.678(3)	Te(2)−Cl(2)	2.672(3)
Te(1)−S(1)	2.518(3)	Te(2)−S(3)	2.509(3)
Te(1)−C(1)	2.13(1)	Te(2)−C(6)	2.13(1)
Te(1)−C(2)	2.132(9)	Te(2)−C(7)	2.16(1)
Te(1)−S(2)	3.292(3)	Te(2)−S(4)	3.210(3)
Te(1)--Cl(1)[a]	3.456(3)	Te(2)--Cl(2)″	3.647(3)
S(1)−C(3)	1.73(1)	S(3)−C(8)	1.73(1)
S(2)−C(3)	1.64(1)	S(4)−C(8)	1.64(1)
O(1)−C(3)	1.32(1)	O(2)−C(8)	1.32(1)
O(1)−C(4)	1.46(1)	O(2)−C(9)	1.50(2)
C(4)−C(5)	1.49(1)	C(9)−C(10)	1.40(2)
Te(1)--Te(1)[a]	5.127(1)	Te(2)−Te(2)[b]	6.110(1)
Te(1)--Te(1)[b]	5.127(1)	Te(2)−Te(2)[a]	6.110(1)
Cl(1)−Te(1)−S(1)	168.48(9)	Cl(2)−Te(2)−S(3)	172.7(1)
Cl(1)−Te(1)−C(1)	84.4(3)	Cl(2)−Te(2)−C(6)	84.4(3)
Cl(1)−Te(1)−C(2)	82.8(3)	Cl(2)−Te(2)−C(7)	86.9(3)
S(1)−Te(1)−C(1)	91.4(3)	S(3)−Te(2)−C(6)	90.4(3)
S(1)−Te(1)−C(2)	87.1(3)	S(3)−Te(2)−C(7)	88.5(3)
C(1)−Te(1)−C(2)	97.0(4)	C(6)−Te(2)−C(7)	96.0(4)
Cl(1)−Te(1)−S(2)	128.63(8)	Cl(2)−Te(2)−S(4)	121.82(9)
S(1)−Te(1)−S(2)	60.59(8)	S(3)−Te(2)−S(4)	62.01(9)
C(1)−Te(1)−S(2)	79.5(3)	C(6)−Te(2)−S(4)	80.0(3)
C(2)−Te(1)−S(2)	147.2(3)	C(7)−Te(2)−S(4)	150.1(3)
Cl(1)−Te(1)--Cl(1)[a]	102.55(8)	Cl(2)−Te(2)--Cl(2)[b]	98.41(5)
S(1)−Te(1)--Cl(1)[a]	79.67(8)	S(3)−Te(2)--Cl(2)[b]	172.7(1)
C(1)−Te(1)--Cl(1)[a]	167.0(3)	C(6)−Te(2)--Cl(2)[b]	84.4(3)
C(2)−Te(1)--Cl(1)[a]	73.4(3)	C(7)−Te(2)--Cl(2)[b]	86.9(3)
S(2)−Te(1)--Cl(1)[a]	103.79(7)	S(4)−Te(2)--Cl(2)[b]	121.82(9)
Te(1)−S(1)−C(3)	98.8(2)	Te(2)−S(3)−C(8)	96.6(4)
S(1)−C(3)−S(2)	125.8(6)	S(3)−C(8)−S(4)	125.9(7)
S(1)−C(3)−O(1)	109.0(7)	S(3)−C(8)−O(2)	108.1(8)
S(2)−C(3)−O(1)	125.3(8)	S(4)−C(8)−O(2)	125.9(9)
C(3)−O(1)−C(4)	120.3(8)	C(8)−O(2)−C(9)	121(1)
O(1)−C(4)−C(5)	108.4(9)	O(2)−C(9)−C(10)	110(1)
Te(1)−Cl(1)[a]−Te(1)[a]	112.8(1)	Te(2)−Cl(2)[b]−Te(2)[b]	150.1(1)
Te(1)−Cl(1)−Te(1)[b]	112.8(1)	Te(2)−Cl(2)−Te(2)[a]	150.1(1)

[a] $x - 1/2, 1/2 - y, z$. [b] $1/2 + x, 1/2 - y, z$.

(24) Least-squares: Function minimized: $\sum w(|F_o| - |F_c|)^2$, where $w = 4F_o^2/\sigma^2(F_o^2)$, $\sigma^2(F_o^2) = [S^2(C + R^2B) + (pF_o^2)^2]/Lp^2$, S = scan rate, C = total integrated peak count, R = ratio of scan time to background counting time, Lp = Lorentz−polarization factor, and $p = p$ factor.
(25) Standard deviation of an observation of unit weight: $[\sum w(|F_o| - |F_c|)^2/(N_o - N_v)^{1/2}$, where N_o = number of observations and N_v = number of variables.
(26) Cromer, D. T.; Waber, J. T. *International Tables for X-ray Crystallography*; The Kynoch Press: Birmingham, England, 1974; Vol. IV, Table 2.2 A.
(27) Ibers, J. A.; Hamilton, W. C. *Acta Crystallogr*. **1964**, *17*, 781.
(28) Cromer, D. T. *International Tables for X-ray Crystallography*; The Kynoch Press: Birmingham, England, 1974; Vol. IV, Table 2.3.1.
(29) TEXSAN-TEXRAY *Structure Analysis Package*; Molecular Structure Corp.: Woodlands, TX, 1985.
(30) Pauling, L. *J. Am. Chem. Soc.* **1947**, *69*, 542. Pauling, L. *The Nature of the Chemical Bond*, 3rd ed.; Cornell University Press: Ithaca, NY, 1960; p 255.

Table 5. Important Interatomic Distances (Å) and Angles (deg) for $Me_2TeI[S_2CO(i\text{-}Pr]$ (**9**)

Te(1)−I(1)	3.049(1)	Te(2)−I(2)	3.071(1)
Te(1)−S(1)	2.517(3)	Te(2)−S(3)	2.531(3)
Te(1)−C(1)	2.14(1)	Te(2)−C(7)	2.13(1)
Te(1)−C(2)	2.14(1)	Te(2)−C(8)	2.14(1)
Te(1)−S(2)	3.215(4)	Te(2)−S(4)	3.169(3)
Te(1)--I(2)	3.766(1)	Te(2)--I(1)	3.766(1)
S(1)−C(3)	1.75(1)	S(3)−C(9)	1.74(1)
S(2)−C(3)	1.62(1)	S(4)−C(9)	1.64(1)
O(1)−C(3)	1.34(1)	O(2)−C(9)	1.31(1)
O(1)−C(4)	1.49(1)	O(2)−C(10)	1.50(1)
C(4)−C(5)	1.49(2)	C(10)−C(11)	1.47(2)
C(4)−C(6)	1.46(2)	C(10)−C(12)	1.49(2)
Te(1)--Te(2)	4.597(1)	Te(2)--Te(1)	4.597(1)
Te(1)--Te(1)[a]	6.584(2)	Te(2)−Te(2)[b]	6.561(2)
I(1)−Te(1)−S(1)	172.10(9)	I(2)−Te(2)−S(3)	176.43(9)
I(1)−Te(1)−C(1)	86.3(3)	I(2)−Te(2)−C(7)	85.7(4)
I(1)−Te(1)−C(2)	87.2(4)	I(2)−Te(2)−C(8)	89.4(4)
S(1)−Te(1)−C(1)	93.7(4)	S(3)−Te(2)−C(7)	92.0(4)
S(1)−Te(1)−C(2)	85.0(4)	S(3)−Te(2)−C(8)	88.1(4)
C(1)−Te(1)−C(2)	99.8(5)	C(7)−Te(2)−C(8)	95.8(5)
I(1)−Te(1)−S(2)	125.63(8)	I(2)−Te(2)−S(4)	119.80(9)
S(1)−Te(1)−S(2)	62.2(1)	S(3)−Te(2)−S(4)	62.50(9)
C(1)−Te(1)−S(2)	83.1(4)	C(7)−Te(2)−S(4)	82.5(3)
C(2)−Te(1)−S(2)	147.1(4)	C(8)−Te(2)−S(4)	150.4(4)
I(1)−Te(1)--I(2)	92.93(4)	I(2)−Te(2)--I(1)	90.64(3)
S(1)−Te(1)--I(2)	87.55(9)	S(3)−Te(2)--I(1)	91.33(9)
C(1)−Te(1)--I(2)	175.9(4)	C(7)−Te(2)--I(1)	173.2(3)
C(2)−Te(1)--I(2)	84.2(4)	C(8)−Te(2)--I(1)	78.4(4)
S(2)−Te(1)--I(2)	94.12(8)	S(4)−Te(2)--I(1)	104.35(8)
Te(1)−S(1)−C(3)	95.5(4)	Te(2)−S(3)−C(9)	95.8(4)
S(1)−C(3)−S(2)	127.1(8)	S(3)−C(9)−S(4)	125.0(7)
S(1)−C(3)−O(1)	106(1)	S(3)−C(9)−O(2)	108.8(8)
S(2)−C(3)−O(1)	126(1)	S(4)−C(9)−O(2)	126.2(8)
C(3)−O(1)−C(4)	121(1)	C(9)−O(2)−C(10)	120.0(9)
O(1)−C(4)−C(5)	108(1)	O(2)−C(10)−C(11)	109(1)
O(1)−C(4)−C(6)	105(1)	O(2)−C(10)−C(12)	104(1)
C(5)−C(4)−C(6)	114(2)	C(11)−C(10)−C(12)	113(1)
Te(1)--I(2)−Te(2)	83.84(3)	Te(2)--I(1)−Te(1)	82.38(3)
Te(1)−I(1)--Te(2)	82.38(3)	Te(2)−I(2)--Te(1)	83.84(3)

[a] $2-x, 2-y, -z$. [b] $2-x, 1-y, -z$.

to interatomic distances for the much longer secondary interactions or partial bonds involving Te and S should utilize percentage differences "normalized" to 1.54 as follows rather than absolute differences. Pauling's relationship, which can written as $n = 10^X$, where $X = (d - d_n)/0.6$, can be modified to allow for percentage differences "normalized" to 1.54 to give $X = [1.54(d - d_n)/d]/0.6$ or $X = 2.57(d - d_n)/d$. It is reasonable to use 2.63 Å as the appropriate length for a Te−S single bond in these compounds because it is typical of the average bond length of many Me_2TeL_2 species, where L is a dithio ligand. Based on this assumption, typical calculated values of the lengths of Te--S partial bonds for various values of n are as follows: 2.63 ($n = 1.0$), 2.75 (0.75), 2.94 (0.50), 3.25 (0.25), and 3.66 Å ($n = 0.10$). Similarly, based on the assumption that the appropriate Te−Cl and Te−I single bond lengths are those found in the corresponding Me_2TeX_2 compounds of 2.51 and 2.92 Å, respectively, for X = Cl and I, typical calculated values of the lengths of Te--X partial bonds for various values of n are as follows: for Te--Cl, 2.51 ($n = 1.0$), 2.63 (0.75), 2.81 (0.50), 3.11 (0.25) and 3.51 Å ($n = 0.10$); for Te--I, 2.92 ($n = 1.0$), 3.06 (0.75), 3.27 (0.50), 3.62 (0.25), and 4.09 Å ($n = 0.10$). All of these values are compatible with the sum of the van der Waals radii of the appropriate atoms[31] and may even be low estimates of bond orders compared to those that may be calculated by an alternative method suggested recently.[32]

Normal Coordinate Analysis. The calculations were only carried out on the methylxanthate derivatives, in part because the focus of our interest was the vibrations involving the S_2COC core and in part because of limitations on the number of atoms in the molecules that could be handled. The molecules $Me_2TeX[S_2COMe]$, where X = Cl, Br, and I, were assumed to be in the C_s point group with dimensions based on the molecular structures of **2** and **9**. An IBM compatible 460 Series PC was used for the normal coordinate analysis using the latest update of the program SOTONVIB, which is a modified version of GMAT and FPERT described by Schachtschneider,[33] supported by the program MCART.[34] The experimental and calculated frequencies, partial assignments of the fundamental modes and potential energy distribution (PED) among the force constants are given for $Me_2TeBr[S_2COMe]$ in

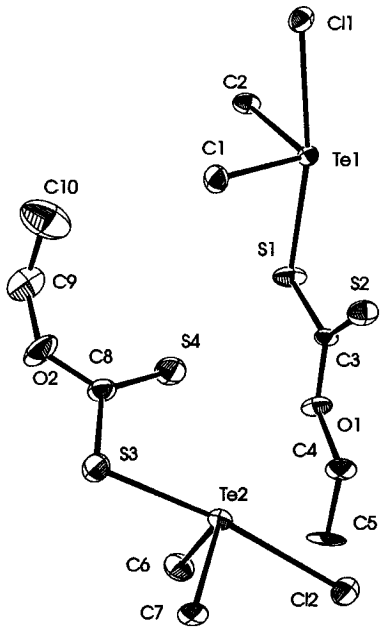

Figure 1. ORTEP plot of the two molecules in the asymmetric unit of $Me_2TeCl[S_2COMe]$ **(2).** The atoms are drawn with 25% probability ellipsoids. Hydrogen atoms are omitted for clarity.

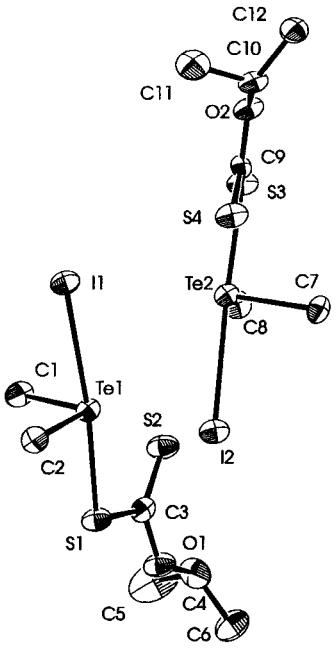

Figure 2. ORTEP plot of the two molecules in the asymmetric unit of $Me_2TeI[S_2CO(i\text{-}Pr)$ **(9).** The atoms are drawn with 25% probability ellipsoids. Hydrogen atoms are omitted for clarity.

(31) Pauling, L. *The Nature of the Chemical Bond*, 3rd ed.; Cornell University Press: Ithaca, NY, 1960; p 260. Bondi, A. *J. Phys. Chem.* **1964**, *68*, 441.

(32) Robinson, E. A. *Can. J. Chem.* **1992**, *70*, 1696 and references therein.

(33) Schachtschneider, J. H. *Vibrational Analysis of Polyatomic Molecules VI;* Project No. 31 450. December 1964. Tech. Report No. 57−65; Shell Development Co.: Emeryville, CA, 1964.

(34) MCART may be obtained directly from T. R. Gilson, Department of Chemistry, The University, Southampton, England.

Table 6. Selected Features (cm^{-1}) and Their Assignments in the Vibrational Spectra of Compounds **1**−**3**[a,b]

$Me_2ClTe[S_2COMe]$ **(1)**		$Me_2TeCl[S_2COEt]$ **(2)**		$Me_2TeCl[S_2CO(i\text{-}Pr)]$ **(3)**		
IR[c]	Raman[d]	IR[c]	Raman[d]	IR[c]	Raman[d]	assgnts
1209 vs	*f*	1201 vs	*f*	1225 vs	*f*	$\nu(S_2COC)_a$[e]
1152 s	*f*	1110 s	*f*	1087 vs	*f*	$\nu(S_2COC)_b$[e]
1049 vs	1050 (16)	1037 vs	1039 (17)	1025 vs	1024 (25)	$\nu(S_2COC)_c$[e]
901 mw	*f*	894 w	*f*	895 w		$\rho(TeCH_3)$
860 mw	*f*	857 mw	*f*	865 ms	*f*	$\rho(TeCH_3)$
633 w	633 (10)	669 w	673 (6)	*f*	675 (30)	$\nu(S_2COC)_d$[e]
537 w, br	538 (60)	533 vw, br	535 (100)	533 w, br	544 (100)	$\nu(Te-C)_{asym}$
537 w, br	528 (80)	533 vw, br	527 (80)	533 w, br	529 (100)	$\nu(Te-C)_{sym}$
458 m	458 (3)	439 m	441 (4)	453 m	458 (15)	δ(COC)
376 m	379 (100)	360 m	360 (35)	322 s	320 (85)	ν(Te−S)
229 m	228 (40)	232 m	239 (80)	236 ms	227 (90)	υ(Te−Cl)
200 sh	206 (90)	200 sh	212 [40]	202 ms, br	202 [80]	δ(CTeC)
193 s, br	206 (90)	189 s, br	187 [40]	202 ms, br	202 [80]	$\delta(S_2COC)$
132 m	*d*	133 m	*d*	129 mw	130 [80]	$\delta(S_2COC)$

[a] Parentheses denote relative intensities in the Raman effect. [b] Key: s = strong, m = medium, w = weak, sh = shoulder, br = broad, and v = very. [c] Run neat between KBr plates down to 400 cm^{-1} and between polyethylene below 400 cm^{-1}. [d] Run neat in sealed capillaries. [e] In the xanthate salts, KS_2COR, these appear for R = Me at 1187 s, 1109 vs, 1049 vs, 620 (100), 476 (30); for R = Et at 1143 s, 1105 vs, 1050 s, 666 (100), 448 (55); and for R = *i*-Pr at 1135 s, 1084 vs, 1056 vs, 660 (100), 462 (60). [f] Not observed.

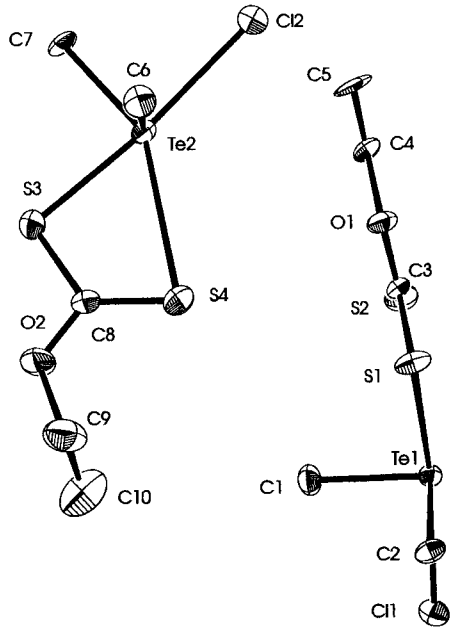

Figure 3. ORTEP plot of the two molecules in the asymmetric unit of $Me_2TeCl[S_2COMe]$ **(2)** with intramolecular interactions included between Te(1)−S(2) and Te(2)−S(4). The atoms are drawn with 25% probability ellipsoids. Hydrogen atoms are omitted for clarity.

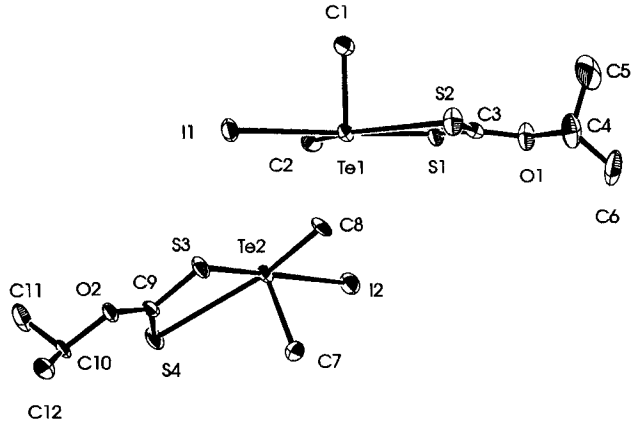

Figure 4. ORTEP plot of the two molecules in the asymmetric unit of $Me_2TeI[S_2CO(i\text{-}Pr)$ **(9)** with intramolecular interactions included between Te(1)−S(2) and Te(2)−S(4). The atoms are drawn with 25% probability ellipsoids. Hydrogen atoms are omitted for clarity.

Table 9 along with those for $Me_2TeCl[S_2COMe]$ and $Me_2TeI[S_2COMe]$ below 600 cm^{-1}. The values of the force constants are given in Table 10.

Results and Discussion

A variety of halodimethyltellurium(IV) *O*-alkyl dithiocarbonate derivatives can be prepared by the addition of an equimolar amount of the potassium salt of *O*-methyl, *O*-ethyl, or *O*-isopropyl dithiocarbonic acid to the appropriate dimethyltellurium dihalide in accord with the general equation

$$Me_2TeX_2 + KS_2COR = Me_2TeX[S_2COR] + KX \quad (1)$$

X = Cl, Br, or I; R = Me, Et, or *i*-Pr

With the exception of $Me_2TeI[S_2COMe]$ (**7**), all of these halo derivatives are fairly stable to atmospheric oxygen and moisture in the sense that they can be handled in the open air rather than under nitrogen and can be stored in closed vials without prior evacuation. As a precaution, the compounds were stored successfully for extended periods at −6 °C, even though all except **7** appeared to be stable at room temperature. The compounds are soluble in common organic solvents such as C_6H_6, $CHCl_3$, and CH_2Cl_2, but in solution they gradually undergo disproportionation to the dihalide and the bis derivative with the latter then undergoing reductive elimination.[19]

$$2Me_2TeX[S_2COR] \rightarrow Me_2Te[S_2COR]_2 + Me_2TeX_2 \quad (2)$$

$$Me_2Te[S_2COR]_2 \rightarrow Me_2Te + ROCS_2S_2COR \quad (3)$$

The decomposition occurs most readily with compound **7**, which cannot be isolated as a solid and even before the addition of solvent shows signs of decomposition within 1−2 h at room temperature.

Molecular Structures of $Me_2TeCl[S_2COEt]$ (2) and $Me_2TeI[S_2CO(i\text{-}Pr)]$ (9). Chlorodimethyl(*O*-ethyl dithiocarbonato)-tellurium(IV) (**2**) and iododimethyl(*O*-isopropyl dithiocarbonato)-tellurium(IV) (**9**) crystallize in the space groups $P2_1/a$ and $P\bar{1}$, respectively. In both **2** and **9** there are two molecules in the asymmetric unit as can be seen in the ORTEP diagrams, which are presented in Figures 1 and 2. The orientations were chosen so that in each case one of the molecules of the asymmetric unit is displayed in the conventional projection that shows the

Table 7. Selected Features and Their Assignments in the Vibrational Spectra of Compounds **4**−**6**[a,b]

$Me_2BrTe[S_2COMe]$ **(4)**		$Me_2TeBr[S_2COEt]$ **(5)**		$Me_2TeBr[S_2CO(i\text{-}Pr)]$ **(6)**		
IR[c]	Raman[d]	IR[c]	Raman[d]	IR[c]	Raman[d]	assgnts
1208 s	*f*	1200 vs	*f*	1232 vs	*f*	$\nu(S_2COC)_a$[e]
1145 ms	*f*	1102 s	*f*	1086 vs	*f*	$\nu(S_2COC)_b$[e]
1043 vs	1040 (5)	1033 vs	1036 (15)	1019 vs	1027 (20)	$\nu(S_2COC)_c$[e]
895 vw	*f*	901 w	*f*	893 mw		$\rho(TeCH_3)$
858 mw	*f*	854 mw	*f*	855 mw	*f*	$\rho(TeCH_3)$
624 w	632 (30)	670 vw, sh	674 (9)	668 m	673 (10)	$\nu(S_2COC)_d$[e]
535 vw, br	537 (50)	526 w, br	534 (65)	538 vw, br	534 (60)	$\nu(Te-C)_{asym}$
535 vw, br	526 (85)	526 w, br	524 (100)	538 vw, br	527 (55)	$\nu(Te-C)_{sym}$
452 mw	450 (5)	435 m	439 (9)	454 m	458 (5)	δ(COC)
374 m	374 (100)	360 s	360 (35)	322 m	323 (100)	ν(Te−S)
200 s	199 (80)	189 m	209 (30)	200 w	200 (30)	$\delta(S_2COC)$
198 sh	199 (80)	189 m	192 (30)	190 w	191 (2)	δ(CTeC)
148 s	148 (60)	136 s	144 (30)	135 m	134 (80)	ν(Te-Br)
120 ms	125 (30)	114 ms	115 (45)	113 m	123 (50)	$\delta(S_2COC)$

[a] Parentheses denote relative intensities in the Raman effect. [b] Key: s = strong, m = medium, w = weak, sh = shoulder, br = broad, and v = very. [c] Run neat between KBr plates down to 400 cm^{-1} and between polyethylene below 400 cm^{-1}. [d] Run neat in sealed capillaries. [e] In the xanthate salts, KS_2COR, these appear for R = Me at 1187 s, 1109 vs, 1049 vs, 620 (100), 476 (30); for R = Et at 1143 s, 1105 vs, 1050 s, 666 (100), 448 (55); for R = *i*-Pr at 1135 s, 1084 vs, 1056 vs, 660 (100), 462 (60). [f] Not observed.

Table 8. Selected Features and Their Assignments in the Vibrational Spectra of Compounds **7**−**9**[a,b]

$Me_2ITe[S_2COMe]$ **(7)**		$Me_2TeI[S_2COEt]$ **(8)**		$Me_2TeI[S_2CO(i\text{-}Pr)]$ **(9)**		
IR[c]	Raman[d]	IR[c]	Raman[d]	IR[c]	Raman[d]	assgnts
1206 s	*f*	1201 vs	*f*	1222 vs	*f*	$\nu(S_2COC)_a$[e]
1143 s	*f*	1106 s	*f*	1083 vs	*f*	$\nu(S_2COC)_b$[e]
1045 vs	1040 (1)	1034 vs	1037 (14)	1019 vs	1026 (6)	$\nu(S_2COC)_c$[e]
895 w	*f*	897 w	*f*	893 m		$\rho(TeCH_3)$
860 mw	*f*	848 mw	*f*	847 mw	*f*	$\rho(TeCH_3)$
670 mw	671 (2)	669 vw	673 (6)	664 m	673 (5)	$\nu(S_2COC)_d$[e]
532 vw, br	524 (10)	524 w, br	528 (45)	521 vw, br	526 (18)	$\nu(Te-C)_{asym}$
532 vw, br	524 (10)	524 w, br	518 (60)	521 vw, br	518 (20)	$\nu(Te-C)_{sym}$
450 m	*f*	436 m	437 (6)	449 m	464 (5)	δ(COC)
364 ms	368 (5)	356 m	356 (50)	315 m	318 (90)	ν(Te−S)
190 s, br	193 (7)	182 m, br	188 (25)	201 m,br	202 (30)	$\delta(S_2COC)$
190 s, br	193 (7)	182 m, br	188 (25)	201 m,br	202 (30)	δ(CTeC)
137 s, br	148 (10)	153 m	153 (25)	154 s	154 (80)	$\delta(S_2COC)$
110 m, sh	115 (100)	103 m	115 (100)	104 m	116 (100)	ν(Te−I)

[a] Parentheses denote relative intensities in the Raman effect. [b] Key: s = strong, m = medium, w = weak, sh = shoulder, br = broad, and v = very. [c] Run neat between KBr plates down to 400 cm^{-1} and between polyethylene below 400 cm^{-1}. [d] Run neat in sealed capillaries. [e] In the xanthate salts, KS_2COR, these appear for R = Me at 1187 s, 1109 vs, 1049 vs, 620 (100), 476 (30); for R = Et at 1143 s, 1105 vs, 1050 s, 666 (100), 448 (55); and for R = *i*-Pr at 1135 s, 1084 vs, 1056 vs, 660 (100), 462 (60). [f] Not observed.

immediate environment about tellurium as a saw horse structure typical of tellurium(IV) compounds in which the lone pair is assumed to be stereochemically active and occupying an equatorial position in a distorted trigonal bipyramid. Thus for both $Me_2TeCl[S_2COEt]$ (**2**) and $Me_2TeI[S_2CO(i\text{-}Pr)]$ (**9**) in Figures 1 and 2, respectively, the lone pair can be visualized as taking up the position indicated approximately by the label Te(1). The two methyl groups occupy the other two equatorial positions, the C−Te−C angles of 97.0(4) and 96.0(4)° being essentially unchanged from the value in $Me_2Te[S_2COEt]_2$ of 96.2(2)°.[19] The Te−C bond lengths are also essentially the same in **2** and **9**. The axial positions are occupied by one of the sulfur atoms of the dithiocarbonate group and the halogen atom, the average Cl−Te−S angles being 168.48(9) and 172.7(1)° in **2** and 172.10(9) and 176.43(9)° in **9** compared with 166.39(5)° in $Me_2Te[S_2COEt]_2$.[19] The halide is in essence replacing the second dithiocarbonate group in $Me_2Te[S_2COEt]_2$, where the two Te−S bonds lengths were very different. There was no close contact between the sulfur atom of the shorter Te−S bond (2.590(2) Å) and an adjacent tellurium atom but the sulfur atom of the longer Te−S bond (2.667(2) Å) was associated with an intermolecular Te--S′ interaction of 3.814(2) Å. There are no similar close intermolecular Te--S′ contacts in **2** or **9**. However, there are intramolecular Te--S interactions, with average lengths of 3.25(6) and 3.19(3) Å for **2** and **9,** respectively, which are shorter than those in the *bis* compound[19] and correspond to approximate Pauling partial bond orders of 0.25 and 0.28. This suggests that they should be included as part of the coordinating sphere around tellurium, and indeed the structure of $Me_2Te[S_2COMe]_2$ has been described as a pseudo pentagonal bipyramid rather than a trigonal bipyramid for the same reason.[2] The projections in Figures 3 and 4 have been selected to demonstrate that the coordination sphere about tellurium can be described as square pyramidal, with the carbon atom of one of the methyl groups, both sulfur atoms and the halogen atom being essentially co-planar and the second methyl group being at right angles to that plane. Thus for $Me_2TeCl[S_2COEt]$ (**2**), C(3), S(1), S(2), and Cl(1) form a plane (mean deviation from plane is 0.017 Å) with Te(1) just below the plane (0.15(1) Å) and with C(1) taking up the axial position (1.93(1) Å above the plane) and C(7), S(3), S(4), and Cl(2) form a plane (mean deviation from plane is 0.009) with Te(2) just below the plane (−0.14(1) Å) and with C(6) taking up the axial position (1.95(1) Å above the plane). In $Me_2TeI[S_2CO(i\text{-}Pr)]$ (**9**), C(3), S(1), S(2), and I(1) form a plane (mean deviation from plane is 0.007 Å) with Te(1) only just below the plane (−0.03(1) Å) and with C(1) again taking up the axial position (2.07(1) Å above the plane) and C(7), S(3), S(4), and Cl(2) form a plane (mean deviation from plane is 0.015) with Te(2) again essentially also in the plane (−0.07(1) Å) with C(6) taking up the axial position (2.05(1) Å above the

Table 9. Experimental and Calculated Values of the Wavenumbers and Partial Assignment of the Fundamentals and Potental Energy Distributions (PED) Among the Force Constants for the Vibrational Spectrum of $Me_2TeBr[S_2COMe]$, along with Comparisons for $Me_2TeCl[S_2COMe]$ and $Me_2TeI[S_2COMe]$ below 600 cm^{-1} [a]

IR	Raman	calcd	assigmt	PED[b,c]
3015 m	*d*	3019	OCH_3 str	99 (OC−H)
3015 m	*d*	3018	OCH_3 str	99 (OC−H)
2992 m	*d*	3016	$TeCH_3$ str	100 (TeC−H)
2992 m	*d*	3015	$TeCH_3$ str	100 (TeC−H)
2992 m	*d*	3015	$TeCH_3$ str	100 (TeC−H)
2992 m	*d*	3015	$TeCH_3$ str	100 (TeC−H)
2934 m	*d*	2901	OCH_3 str	99 (OC−H)
2934 m	*d*	2899	$TeCH_3$ str	100 (TeC−H)
2934 m	*d*	2899	$TeCH_3$ str	100 (TeC−H)
1435 m	1439 (5)	1434	OCH_3 bend	58 (HCO) + 28 (HCH)O + 13 (H_3C−O)
1390 m, sh	*e*	1342	OCH_3 bend	78 (HCH)O + 22 (HCO)
1390 m, sh	*e*	1340	OCH_3 bend	82 (HCH)O + 18 (HCO)
1315 w	*e*	1281	$TeCH_3$ bend	41 (TeCH) + 54 (HCH)Te
1315 w	*e*	1281	$TeCH_3$ bend	41 (TeCH) + 54 (HCH)Te
1261 m	1238 (10)	1253	$TeCH_3$ bend	91 (HCH)Te
1261 m	1238 (10)	1253	$TeCH_3$ bend	91 (HCH)Te
1261 m	1224 (5)	1253	$TeCH_3$ bend	91 (HCH)Te
1261 m	1224 (5)	1253	$TeCH_3$ bend	91 (HCH)Te
1208 s	*e*	1214	S_2COC *a*-str	20 (C═S) + 19 (C−O) + 21 (COC) + 13 (HCO)
1145 ms	*e*	1145	S_2COC *b*-str	59 (C−O) + 26 (C−STe) + 15 (H_3C−O)
1091 ms	1049 (10)	1061	OCH_3 rock	80 (HCO) + 18 (HCH)O
1043 vs	1040 (5)	1045	S_2COC *c*-str	31 (C═S) + 19 (C−STe) + 32 (HCO)
940 sh	930 (12)	947	and OCH_3 rock	59 (H_3C−O) + 23 (HCO) + 10 (C−STe)
895 vw	e	860	$TeCH_3$ rock	91 (TeCH)
858 mw	e	855	$TeCH_3$ rock	91 (TeCH)
858 mw	e	855	$TeCH_3$ rock	91 (TeCH)
820 w	e	855	$TeCH_3$ rock	91 (TeCH)
624 w	632 (30)	635	S_2COC *d*-str	49 (C═S) + 17 (COC)
535 vw, br	537 (50)	535	Te−C asymm str	95 (Te−C)
525 vw, br	526 (85)	526	Te−C symm str	95 (Te−C)
452 mw	450 (5)	448	COC bend	42 (COC) + 32 (C−STe)
374 m	374 (100)	372	Te−S str	85 (Te−S)
280 w	280 (20)	274	C═S wag	98 (OPLA)CS
200 s	199 (80)	199	S_2COC def	43 (SCS) + 31 (SCO) + 12 (COC)
198 sh	199 (80)	197	C−Te−C bend	99 (CTeC)
148 s	148 (60)	153	Te−Br str	78 (Te−Br)
120 ms	125 (30)	120	S_2COC def	25 (OCS)Te + 24 (SCO) + 22 (SCS) + 17 (Te−Br)
			$Me_2TeCl[S_2COMe]$	
537 w, br	538 (60)	537	Te−C asymm str	95 (Te−C)
537 w, br	528 (60)	528	Te−C symm str	95 (Te−C)
458 m	458 (3)	448	COC bend	42 (COC) + 32 (C−STe)
376 m	379 (100)	379	Te−S str	86 (Te−S)
285 vw	277 (20)	274	C═S wag	98 (OPLA)CS
229 m	228 (40)	228	Te−Cl str	90 (TeCl)
200 sh	206 (90)	199	C−Te−C bend	99 (CTeC)
193 s, br	206 (90)	195	S_2COC def	36 (SCS) + 34 (SCO) + 12 (COC)
132 m	*f*	125	S_2COC def	31 (SCO) + 30 (OCS)Te + 25 (SCS)
			$Me_2TeI[S_2COMe]$	
532 vw, br	524 (10)	527	Te−C asymm str	95 (Te−C)
532 vw, br	524 (10)	518	Te−C symm str	95 (Te−C)
450 m	f	448	COC bend	42 (COC) + 32 (C−STe)
364 ms	368 (5)	367	Te−S str	87 (Te−S)
280 vw	281 (5)	274	C═S wag	98 (OPLA)CS
190 s, br	193 (7)	198	S_2COC def	43 (SCS) + 32 (SCO) + 12 (OCO)
190 s, br	193 (7)	196	C−Te−C bend	99 (CTeC)
137 s, br	148 (10)	137	S_2COC def	43 (Te−I) + 23 (SCO) + 17 (OCS)Te
110 m, sh	115 (100)	111	Te−I str	54 (Te−I) + 13 (SCS) + 13 (OCS)Te + 11 (SCO)

[a] The assignments and potential energy distributions are the same for all three molecules above 600 cm^{-1}. [b] Only contributions greater than 10% are listed. [c] Contributions greater than 2% from the nondiagonal force constants (no. 19−23 in Table 10) are as follows for S_2COC *a*-stretch, −3.5(19) −7.9(22); S_2COC *b*-stretch, −6.0(19) −8.1(22); S_2COC *c*-stretch, −7.3(19) −5.1(21) −2.0(22) + 4.0(23); S_2COC *d*-stretch, 5.2(19) + 6.3(21). [d] The Raman spectra were only scanned below 1500 cm^{-1}. [e] Not observed. [f] Cut off below 200 cm^{-1}.

plane). The lone pair still appears to be stereochemically active in occupying the position trans to the axial methyl group to give a pseudooctahedral arrangement. The average Te−S bond length in both **2** and **9** are significantly shorter at 2.514(6) and 2.542(9) Å, respectively, than even the shorter bond in $Me_2Te[S_2COEt]_2$.[19] These correspond to bond orders of 1.30 and 1.22, respectively, relative to a bond order of 1.0 in the *bis* compound, suggesting a significant increase in the π-character of the Te−S bond when it is not mutually trans with a second Te−S bond.

By contrast, the average Te−Cl bond length of 2.675(4) Å in **2** is considerably longer than that of 2.51(4) Å in α-Me_2TeCl_2.[35] Similarly the average Te−I bond length of 3.06(2) Å in **9** can be compared to a range of 2.885(3)−2.994(3) Å in

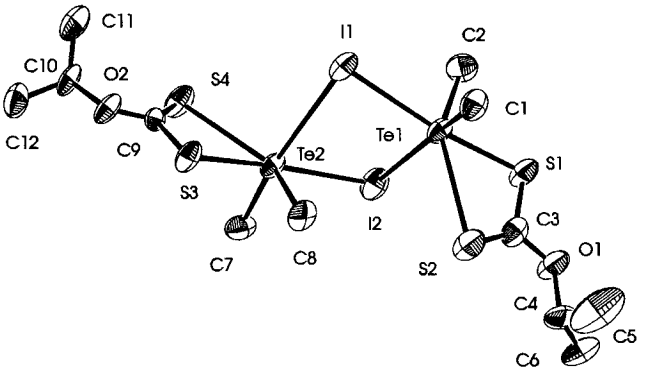

Figure 5. ORTEP plot of the two molecules in the asymmetric unit of $Me_2TeI[S_2CO(i\text{-}Pr)$ **(9)** with both inter- and intramolecular interactions included to give an apparent dimeric species. The atoms are drawn with 25% probability ellipsoids. Hydrogen atoms are omitted for clarity.

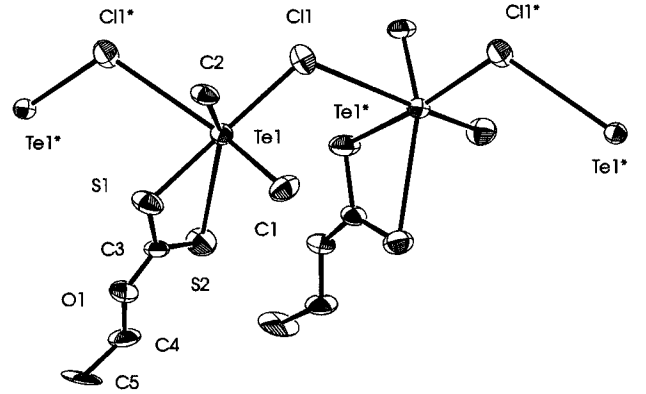

Figure 6. ORTEP plot of a sequence of one of the two molecules in the asymmetric unit of $Me_2TeCl[S_2COMe]$ **(2)** with inter- and intramolecular interactions included to give a pseudopolymer. The atoms are drawn with 25% probability ellipsoids. Hydrogen atoms are omitted for clarity.

α-Me_2TeI_2.[36] In both **2** and **9**, there are intermolecular interactions resulting in the formation of unsymmetrical Te−X--Te′ bridges. The Te--X′ intermolecular distances of 3.456(3) and 3.647(3) for Te---Cl′ in **2** and 3.766(1) Å for Te--I′ in **9** are essentially the same as, or possibly even shorter than, the average distances in the Me_2TeX_2 species of 3.50 and 3.88 Å, respectively, for X = Cl and I. As with the dihalides and $Me_2TeI[SCONEt_2]$ derivative,[12] the I−Te--I′ and Te−I--Te′ angles in $Me_2TeI[S_2COEt]$ (**9**) are both close to 90°, so the bridging system essentially forms a rectangle to give a dimeric species (Figure 5), with a Te(1)--Te(2) distance of 4.597(1) Å. The inclusion of the Te--I′ interaction indicates that the orientation about tellurium is that of a distorted octahedron in which the lone pair is apparently inert. The Te−X and Te--X′ bonds are thus essentially *cis*, at angles of 92.93(4) and 90.64(3)° for the two molecules of **9** in the asymmetric unit. If the bond order is based on the assumption that the average Te−I bond distance in Me_2TeI_2 corresponds to a bond order of 1.0, then the Pauling partial bond orders of Te−I and Te--I′ in **9** are 0.75 and 0.18, respectively. The corresponding Te−Cl and Te--Cl′ bond orders in $Me_2TeCl[S_2COEt]$ (**2**) are 0.68 and 0.10, respectively, but in contrast to **9**, the Te--Cl′ interactions result in a pseudopolymer. The zigzag Te−Cl--Te′ bridge has an angle of 112.8(1)° in chains of one the molecules of the asymmetric unit (Figure 6). The corresponding Te−Cl--Te′ angle involving the second molecule of the asymmetric unit is 150.1(1)° and the two strands are independent because the closest contact between two Te atoms in different polymer strands is 7.916(1) Å.

The existence of the longer, weaker Te−X bond in **2** and **9** may be attributed, at least in part, to the involvement of the halogen atoms in intermolecular links leading to bridging. However, the shortening of the Te−S bond and lengthening of the Te−X bond is also consistent with a stronger π-contribution to the Te−S bond indicating that the *trans* effect is operative in this main group metal, as was noted for the related monothiocarbamate series.[19]

The terminal or anisobidentate C═S bonds in **2** and **9** are considerably shorter (1.64(1) Å in **2** and 1.63(1) Å in **9**) than the C−STe bonds (1.735(7) Å in **2** and 1.745(7) Å in **9**). These bond lengths are essentially the same as reported for $Me_2Te[S_2COEt]_2$,[19] $Me_2Te[S_2COMe]_2$,[2] or $C_8H_8Te[S_2COEt]_2$.[4] The distortion of the angles around the planar thio-bonded carbon atom is also similar in all of these molecules. The S═C−S and S═C−O angles in **2** and **9**, which average 126.0(9) and 125.8(4)°, respectively, are not only essentially identical but also are considerably larger than the average value of 108(1) for the O−C−S(Te) angles, suggesting similar π-character in the bonds involving the terminal sulfur and oxygen atoms and very little if any in the C−S(Te) bonds. The $O-CS_2$ bond is certainly appreciably shorter (an average of 1.33(5) Å in **2** and **9**) compared to the $O-CH_2$ or O−CH bonds (an average of 1.49(2) Å).

Infrared and Raman Spectra. Selected features in the infrared and Raman spectra and their assignments are given in Table 6 for compounds **1**−**3**, in Table 7 for compounds **4**−**6**, and in Table 8 for compounds **7**−**9**. The assignments are based on those reported previously for the related bis compounds,[19] dihalodimethyl tellurium(IV) compounds,[37] the starting salts, and the most recent attempt at the vibrational analyses of alkyl xanthates[20] along with normal coordinate analyses utilizing the program SOTONVIB.[33] The experimental and calculated frequencies, partial assignments of the fundamental modes and potential energy distributions (PEDs) among the force constants that are given for $Me_2TeBr[S_2COMe]$ in Table 9 along with those for $Me_2TeCl[S_2COMe]$ and $Me_2TeI[S_2COMe]$ below 600 cm^{-1}. The values of the force constants are given in Table 10.

The infrared spectra of dithiocarbonate derivatives, whether it be salts or metal complexes, show three very intense, characteristic peaks within the range 1232−1019 cm^{-1} that have typically been assigned to S_2COC stretching vibrations. These dominate the spectra relative to the peaks assignable to alkyl groups.[38,39] In assigning these modes in the $Me_2Te[S_2COR]_2$ series,[19] we indicated our belief that there was extensive mixing of the stretches so that general assignments as $\nu(S_2COC)_a$, $\nu(S_2COC)_b$ and $\nu(S_2COC)_c$ were more appropriate than specific assignments as $\nu(S_2C-O)$, $\nu(C=S)$ and $\nu(H_3C-O)$. The potential energy distribution among the force constants for the vibrations between 1214 and 947 cm^{-1} (see Table 9) for $Me_2TeBr[S_2COMe]$ are in agreement with this assumption. In terms of diagonal force constants, not only is there considerable mixing involving all four stretching force constants, fc(C═S), fc(C−O), fc(C−STe) and fc(H_3C-O) but also there are contributions from the bending force constants fc(HCO) and fc(COC). In fact one of the OCH_3 rocking modes could be described as a S_2COC stretch and vice versa. The fourth S_2COC stretching vibration, $\upsilon(S_2COC)_d$, which has a substantial contribution from fc(C-

(35) Christofferson, G. D.; Sparks, R. A.; McCullough, J. D. *Acta Crystallogr.* **1958**, *11*, 782.
(36) Chan, Y. Y.; Einstein, F. W. B. *J. Chem. Soc., Dalton Trans.* **1972**, 316.
(37) Hayward, G. C.; Hendra, P. J. *J. Chem. Soc. A* **1969,** 1760.
(38) Drake, J. E.; Mislankar, A. G.; Wong, M. L. Y. *Inorg. Chem.* **1991**, *30*, 2174.
(39) Drake, J. E.; Mislankar, A. G.; Yang, J. *Inorg. Chim. Acta* **1993**, *211*, 37.

Table 10. Values of the Force Constants for $Me_2TeX[S_2COMe]$ (X= Cl, Br, I)[a]

No.	force constant	Me_2TeCl-$[S_2COMe]$	Me_2TeBr-$[S_2COMe]$	Me_2TeI-$[S_2COMe]$
1	C−H	4.840	4.840	4.840
2	C-O	4.902	4.902	4.902
3	H_3C-O	4.679	4.679	4.679
4	C═S	4.351	4.351	4.351
5	C-STe	4.202	4.202	4.202
6	Te−C	2.345	2.325	2.253
7	Te−S	2.025	2.013	1.904
8	Te−X	0.877	0.701	0.647
9	(HCH)Te	0.430	0.430	0.430
10	TeCH	0.572	0.572	0.572
11	(HCH)O	0.480	0.480	0.480
12	HCO	0.798	0.798	0.798
13	COC	1.683	1.683	1.683
14	SCS	0.517	0.517	0.517
15	SCO	0.601	0.601	0.601
16	(OCS)Te	0.148	0.148	0.148
17	(OPLA)CS	0.613	0.613	0.613
18	CTeC	0.779	0.767	0.755
19	C═S/C−STe	0.651	0.651	0.651
20	C−O/C═S	0.803	0.803	0.803
21	C−O/C−S(Te)	0.348	0.348	0.348
22	C−O/O−CH_3	0.647	0.647	0.647
23	C−O/HCO	0.236	0.236	0.236

[a] Units are: mdyn/Å for stretching, mdyn Å for bending and mdyn for stretch−bend interactions.

STe) in its PED, is observed in the region 673−624 cm^{-1} for compounds **1**−**9**, but with less intensity than in the Raman spectra of the salts. The similarity of the location and appearance of the bands in all nine compounds is consistent with the dithiocarbonate groups being attached to tellurium in the same manner in every case, primarily through one strong Te−S bond. Relatively large values for the interaction force constants (no. 19−23) are needed to obtain a reasonable fit between calculated and observed frequencies for all four of the stretching vibrations of the xanthate groups even though their contributions to the potential energy distribution are small, as can be seen from the footnotes in Table 9.

The spectra of all three compounds, **1**−**3**, are very similar in all respects above 600 cm^{-1} and unambiguously assignable, as appropriate, to CH_3 stretching, bending, and rocking modes with values of the force constants (Table 10) being the same and transferrable. The details for the chloride and iodide derivatives are therefore only included in Table 9 for vibrations below 600 cm^{-1}. In compounds **1**−**9**, the asymmetric and symmetric Te−C stretching vibrations are assigned to peaks in the region 544−518 cm^{-1}. These features are weak in the infrared spectra but strong in the Raman effect relative to those of the thio ligand. The values are similar but not identical to those in the corresponding Me_2TeX_2 species,[37] although the relative intensities differ from those of the latter in the Raman effect. The near coincidence of these modes is consistent with a C−Te−C angle close to 90°. It has been noted for other series that as the halogen atom attached to the central atom becomes less electronegative so the bonding of other centrally bonded groups appears to weaken. This is reflected in the slight but general decrease in the Te−CH_3 stretching modes along any series Cl > Br > I and in the slightly decreasing values of the force constants, fc(Te−C), of 2.345, 2.325 and 2.253 mdyn/Å for $Me_2TeX[S_2COMe]$, X = Cl, Br, and I, respectively. The same is true for the force constant fc(Te−S) with values of 2.025, 2.013, and 1.904 mdyn/Å in **1**, **2**, and **3**, respectively. The Te−S stretching vibrations in the range 377−313 cm^{-1} in compounds **1**−**9** are in similar regions to those reported for other Me_2TeXL species[12,14−16] and for the asymmetric stretch in Me_2TeL_2 species,[12−16] where L is a ligand attached to tellurium through a sulfur atom. The CTeC deformation is characteristically observed in the range 189−200 cm^{-1} in all compounds in both the infrared and Raman effect.

By analogy with the spectra of Me_2TeCl_2, Me_2TeBr_2, and Me_2TeI_2,[37] the Te−X stretching vibration might be expected at approximately 260, 160, and 130 cm^{-1}, respectively for X = Cl, Br, and I. Peaks assignable to ν(Te−X) are observed in the range 229−239 cm^{-1} in **1**−**3**, 134−148 cm^{-1} in **4**−**6**, and to 103−106 cm^{-1} in **7**−**9**, which is indicative of a weaker, longer bond in these $Me_2TeX[S_2COR]$ species relative to the corresponding Me_2TeX_2 entities. The values of the force constants, 0.877, 0.701, and 0.647 mdyn/Å for fc(Te−Cl), fc(Te−Br), and fc(Te−I), respectively, for the $Me_2TeX[S_2COMe]$ series are all considerably less than those of fc(Te−S) reflecting the much weaker Te−X bonds. Thus the assignments, supported by the normal coordinate analyses, confirm that the phenomenon of the weaker longer Te−X bond and shorter stronger Te−S bond observed in the X-ray structures of **2** and **9** is a general phenomenon in these mixed halo xanthate derivatives. The value of fc(Te−Cl) can be compared with that of 1.317 mdyn/Å reported for the asymmetric stretch in $XeCl_2$[40] which also has relatively weak bonds. It is noticeable that the Te−Cl stretch is a relatively "pure" mode whereas there is increasing mixing of the force constants for the Te−Br and Te−I stretches with the S_2COC deformation modes. This could account for there being less difference than expected in the appearance of the spectra below 400 cm^{-1} in both the Raman and far infrared spectra.

NMR Spectra. The ^1H, $^{13}C\{H\}$, and ^{125}Te NMR spectra data for compounds **1**−**9** are presented in Table 11. All of the ^1H NMR spectra recorded immediately after dissolution in $CDCl_3$ are consistent with the presence of pure samples of these mixed halogenodithiocarbonate species, with the exception of compound **7**, which even initially has weak signals attributable to decomposition products. The splitting patterns, relative intensities of peaks, and values of the coupling constants are consistent with the formulation $Me_2TeX[S_2COR]$ in all cases. All derivatives show a sharp singlet assignable to the CH_3 group attached to tellurium. There is a progressive shift as the halide changes so that these singlets are seen at 2.78−2.79 ppm for the derivatives where X = Cl, **1**−**3**, at 2.83−2.84 for X = Br, **4**−**6**, and at 2.85−2.87 ppm for X = I, **7**−**9**. The consistency of shift regardless of the nature of the R group and a shift upfield of about 0.35 ppm from that of the starting materials, Me_2TeCl_2 (3.10 ppm), Me_2TeBr_2 (3.26 ppm), and Me_2TeI_2 (3.27 ppm), has been noted for related mixed species.[14−16] The chemical shifts of the protons in the dithiocarbonate are very similar to those in the corresponding bis compounds,[19] so the presence of a halide or another dithiocarbonate is not indicated by any change in the chemical shifts.

In the ^{13}C NMR spectra, the chemical shifts of the ligand methyl, ethyl and isopropyl groups appear at positions very close to those of the starting salts or the related bis compounds. However, the dithiocarbonate carbon, S_2CO, peaks all lie within the range of 215−217 ppm, slightly upfield relative to the values in the corresponding bis compounds whose values range from 218.9 to 221 ppm, and essentially between those of the salts at 233 ppm and the diligands, $ROCS_2S_2COR$, at 207 ppm. It is reasonable to assume that the environment of the S_2CO carbon in the salt would be similar to that of a bidentate ligand and that of the diligands to a monodentate ligand so the ^{13}C NMR is consistent with the environment in compounds **1**−**9**, as well as the bis analogues, being anisobidentate as in the solid state

(40) Nelson, L. Y.; Pimenthal, G. C. *Inorg. Chem.* **1967**, *6*, 1758.

Table 11. 1H, 13C and 125Te NMR Chemical Shifts for the Halodimethyltellurium Dithiocarbonates (**1**−**9**)[a−d]

no.	compd	Te−CH_3 [Te−C]	O-CH_n [O-CH_n]	OC−CH_3 [OC−CH_3]	{^{125}Te} [S_2CO]
1	$Me_2TeCl[S_2COMe]$	2.79	4.10		{587.8}
		(6 H, s)	(3 H, s)		
		[20.25]	[61.77]		[217.67]
2	$Me_2TeCl[S_2COEt]$	2.79	4.54	1.38	{580.3}
		(6 H, s)	(2 H, q, 7.1)	(3 H, t, 7.1)	
		[20.17]	[71.90]	[14.00]	[216.76]
3	$Me_2TeCl[S_2CO(i\text{-}Pr)]$	2.78	5.55	1.34	{577.2}
		(6 H, s)	(1 H, sept, 6.2)	(6 H, d, 6.2)	
		[21.25]	[80.29]	[20.07]	[215.79]
4	$Me_2TeBr[S_2COMe]$	2.83	4.12		{565.6}
		(6 H, s)	(3 H, s)		
		[19.49]	[61.94]		[217.62]
5	$Me_2TeBr[S_2COEt]$	2.83	4.55	1.37	{558.1}
		(6 H, s)	(2 H, q, 7.1)	(3 H, t, 7.1)	
		[19.42]	[72.15]	[13.99]	[216.84]
6	$Me_2TeBr[S_2CO(i\text{-}Pr)]$	2.84	5.57	1.36	{552.9}
		(6 H, s)	(1H, sept, 6.2)	(6 H, d, 6.2)	
		[21.41]	[80.61]	[19.34]	[215.69]
7	$Me_2TeI[S_2COMe]$	2.87	4.12		{535.2}
		(6 H , s)	(3 H, s)		
		[17.95]	[61.96]		[216.37]
8	$Me_2TeI[S_2COEt]$	2.86	4.55	1.39	{528.5}
		(6 H, s)	(2 H, q, 7.1)	(3 H, t, 7.1)	
		[17.86]	[72.16]	[14.06]	[217.44]
9	$Me_2TeI[S_2CO(i\text{-}Pr)]$	2.85	5.58	1.36	{524.7}
		(6 H, s)	(1 H, sept, 6.0)	(6 H, d, 6.0)	
		[21.25]	[80.16]	[17.84]	[216.39]

[a] The spectra were recorded in $CDCl_3$ and reported in ppm from Me_4Si for ^1H and ^{13}C, and from Me_2Te for ^{125}Te. [b] Number of protons, multiplicities (s = singlet; d = doublet; q = quartet; sept = septet) and coupling constants in Hz, are given in parentheses. [c] ^{13}C NMR peaks given in square brackets. [d] Peaks attributable to the corresponding diligands are seen for $[MeOCS_2]_2$ at 4.21 (6 H, s) [61.81 and 208.30]; for $[EtOCS_2]_2$ at 4.66 (4 H, q, 7.0) [71.70], 1.45 (6 H, t, 7.0) [13.75 and 207.50]; and for $[(i\text{-}Pr)OCS_2]_2$ at 4.88 (2 H, sept, 6.2), [71.13], 1.24 (12 H, d, 6.2) [21.97 and 208.00].

structures of **2** and **9**. Peaks due to the methyl carbon atom attached to tellurium show a small steady trend in any $Me_2TeX[S_2COR]$ series as exemplified for the $Me_2TeX[S_2COMe]$ series with values of 20.25, 19.49, and 17.95 ppm respectively for X = Cl, Br, and I.

The ^{125}Te NMR spectra of Me_2TeCl_2, Me_2TeBr_2, Me_2TeI_2, and $Me_2Te[S_2COR]_2$ species have chemical shifts of 733.8, 649.2, 519.6, and an average of 478 ppm, respectively. The effects of the change in substitution are not simply additive; the differences in the chemical shifts along any $Me_2TeX[S_2COR]$ series as Cl is replaced by Br and then I being approximately 23 and 30 ppm, respectively, compared with 85 and 130 ppm for the dihalide series. In other words the chemical shifts for **1**−**9** are much closer to those of $Me_2Te[S_2COR]_2$ compounds than to those of Me_2TeX_2. This may be related to the fact that the Te−S bonds are shorter than in the bis compounds and the Te−X bonds longer than in the dihalides. The difference in the chemical shift of approximately 5 ppm per carbon atom as the alkyl group in the dithiocarbonate changes from Me to Et to *i*-Pr is similar to the bis compounds.

In all compounds **1**−**9**, additional peaks appear in the NMR spectra consistent with the disproportionation of the mixed species to the dihalide and the bisderivative as mentioned at the beginning of this discussion. In general, peaks attributable to Me_2TeX_2 and $Me_2Te[S_2COR]_2$ grow as those attributable to $Me_2TeX[S_2COR]$ decrease in accord with eq 2. The peaks attributable to $Me_2Te[S_2COR]_2$ also start to decrease as peaks attributable to the diligand appear and steadily increase in intensity along with peaks attributable to Me_2Te in accord with eq 3. The progress of disproportionation and reductive elimination are similar regardless of the nature of the R group. However, recording of spectra with time for the $Me_2TeX[S_2COEt]$ gave a quantitative indication that disproportionation took place more readily in the order I > Br > Cl, while reductive elimination was unaffected by the nature of X.

The series of compounds reported herein provide new examples of the strange stereochemistry of tellurium with **2** and **9** providing illustrations of association through secondary interactions leading to quite different supramolecular associations. By contrast, vibrational and NMR spectroscopic results emphasize the similarities of the immediate environment about tellurium, and in solution all species undergo disproportionation and reductive elimination.

Acknowledgment. We wish to thank the Natural Sciences and Engineering Research Council of Canada for financial support and Dr. T. R. Gilson of the University of Southampton for the latest versions of SOTONVIB and MCART. One of us R.R thanks Dayanand College, Ajmer, India, for granting a leave of absence and L.N.K. thanks the former for an NSERC Research Reorientation Associateship.

Supporting Information Available: Tables S1−S5, listing experimental details, anisotropic thermal parameters for non-hydrogen atoms, and final fractional coordinates and thermal parameters for hydrogen atoms (6 pages). Ordering information is given on any current masthead page. Structure factor tables may be obtained directly from the authors.

IC9511736